

## SFM SIGNAL DETECTION AND PARAMETER ESTIMATION BASED ON PULSE-REPETITION-INTERVAL TRANSFORM

*Bin Deng, Yu-Liang Qin, Hong-Qiang Wang, Xiang Li, Lei Nie*

College of Electronic Science and Engineering, National University of Defense Technology, China

### ABSTRACT

A novel algorithm is proposed for detecting and estimating sinusoidal frequency-modulated (SFM) signals based on the pulse-repetition-interval (PRI) transform which is originally used for estimating PRIs of pulse trains. Our algorithm utilizes the resemblance between the spectrum of a SFM signal and a pulse train, and applies the PRI transform to this spectrum. It can detect SFM signals under moderate signal-to-noise ratios, and is also capable of accurately estimating the modulation frequencies even if there are multiple components. The algorithm proposed has been successfully applied to simulated data, and compared with that of the autocorrelation method, showing its superiority.

**Index Terms**— Sinusoidal frequency-modulated (SFM) signal, pulse-repetition-interval (PRI) transform, detection, estimation

### 1. INTRODUCTION

Sinusoidal frequency-modulated (SFM) signals are widely present in radar, speech, sonar and communication. For example, micromotion targets in synthetic aperture radar (SAR) can be characterized by SFM signals in noise and clutter environments [1]. Therefore, study on their detection and estimation is very important. We note that, in reality, detection and estimation can not be strictly distinguished.

A few efforts have been devoted to the detection/estimation of SFM signals. In [2], the time-frequency distribution followed by the Hough transform was proposed to detect SFM signals. The method is sensitive to thresholds and invalid when the signal-to-noise ratio (SNR) is below -10 dB [2]. Also, long computation time is required by the Hough transform. Besides, there also exist a few algorithms for estimating the modulation

frequency. The estimation method based on the time-frequency distribution plus the extended Hough transform [2] is most popular but is subject to high computation complexity. A new basis decomposition method was proposed in [3], which is in effect identical to the maximum likelihood estimation. The method entails searching multiple parameters and therefore introduces significant calculation requirements. The autocorrelation function [4] and the average magnitude difference function can also be used to estimate micro-motion periods or frequencies, but they need long enough signal sequences and are subject to multiple-period errors due to the peak periodicity in the two functions above. The space between spectrum peaks is also utilized for period estimation [5]. It requires high SNR to obtain fine spectra. The cyclic spectral density method [6] dispenses with limitations to the signal length, but it is not suited to multiple components possessing different modulation frequencies.

Herein, we will develop a novel detection and estimation algorithm based on the pulse-repetition-interval (PRI) transform which is originally for estimating PRIs of an interleaved pulse train [7]. We observe the resemblance between SFM-signal spectra and pulse trains, and hence combine the Fourier transform with the PRI transform to realize the detection SFM signals and the estimation of the modulation frequency. The rest of the paper is as follows. In Section 2, the PRI transform is dealt with. In Section 3, the SFM signal model is built, and then a new algorithm is proposed by applying the PRI transform to it. Section 4 provides several results and performance analysis with simulated data. Conclusions are reported in Section 5.

### 2. PRI TRANSFORM [7]

The PRI transform is an ingenious and well-performed algorithm for estimating PRIs of a pulse train, even if the train is a superimposition of several independent radar signals with different PRIs. It is able to suppress the subharmonics appearing in the autocorrelation function.

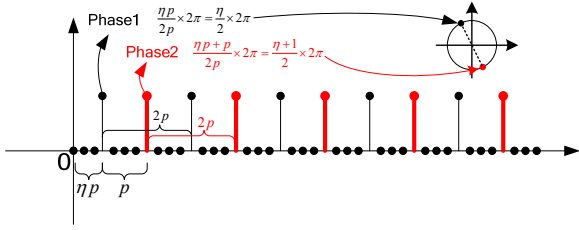


Fig. 1. Pulse train and its decomposition (two sub-pulse-trains as example).

Suppose a pulse train can be modeled as a sum of unit impulses

$$g(t) = \sum_{n=0}^{N-1} \delta(t - t_n) \quad (1)$$

where  $\delta(\cdot)$  is the Dirac delta function,  $t_n$  is the pulse arrival time, and  $N$  is the number of pulses. Define the following integral transform

$$D(\tau) = \int_{-\infty}^{\infty} g(t)g(t+\tau) \exp\left(j2\pi \frac{t}{\tau}\right) dt \quad (2)$$

Clearly, the transform is similar to the complex-valued autocorrelation function, and the difference is that  $g(t)$  in the PRI transform must take on values of zero or a constant (usually one). Substituting (1) into (2) leads to

$$D(\tau) = \sum_{n=1}^{N-1} \sum_{m=0}^{n-1} \delta(\tau - t_n + t_m) \exp\left(j2\pi \frac{t_n}{t_n - t_m}\right) \quad (3)$$

(2) and (3) are named the PRI transform. We can find that a phase term is contained for subharmonic suppression. The locations of the peaks appearing in  $D(\tau)$  indicate the PRI values. The idea of suppressing subharmonics lies in that, for a pulse train containing only one PRI, it can be regarded as one original pulse train, and can also be decomposed into two sub-pulse-trains with the same PRI (two times of the original PRI) but with different phase terms (Fig. 1), or into more such sub-pulse-trains. When the PRI transform is performed, the phase terms from all the sub-pulse-trains are equally spaced at the unit circle and hence can be cancelled out, so the subharmonics are suppressed.

The PRI transform above can be further discretized for realization in computers. It has also been improved for processing pulse jitter [7]. In the following analysis we will make use of the improved version.

### 3. SFM SIGNAL DETECTION AND ESTIMATION USING PRI TRANSFORM

#### 3.1. Signal model

A SFM signal can be expressed by

$$S_{rc}(t_m) = \tilde{\rho} \exp(j2\pi f_0 t_m + jA \cos(\omega_m t_m + \varphi_0)) \quad (4)$$

where  $\tilde{\rho}$  is assumed to be a constant complex factor,  $f_0$  is the fundamental frequency at  $t_m = 0$ ,  $\omega_m$  is the modulation angular frequency,  $f_m = \omega_m / (2\pi)$  is the modulation frequency, and  $A$  is the modulation index.

#### 3.2. Jacobi-Anger expansion

(4) can be expanded by Jacobi-Anger expansion

$$e^{jA \sin \theta} = \sum_{n=-\infty}^{\infty} J_n(A) e^{jn\theta} \quad (5)$$

where  $J_n(\cdot)$  is the  $n$ -th order of first-kind Bessel function.

Substituting (5) into (4) yields

$$\begin{aligned} S_{rc}(t_m) &= \tilde{\rho} \exp(j2\pi f_0 t_m) \exp(jA \sin(\omega_m t_m + \varphi_0 - \pi/2)) \\ &= \tilde{\rho} \exp(j2\pi f_0 t_m) \sum_{n=-\infty}^{\infty} J_n(A) \exp(jn\varphi_0 - jn\pi/2) \exp(jn\omega_m t_m) \end{aligned} \quad (6)$$

Clearly, the signal contains multiple harmonics. Under Carson's rule, the number of the harmonics is

$$N \approx 2|A| + 3 \quad (7)$$

The strength of the harmonics is weighted by Bessel functions. Also, the spacing between their frequencies is  $\omega_m$ , resulting in a comb-shaped spectrum, as Fig. 2 shows.

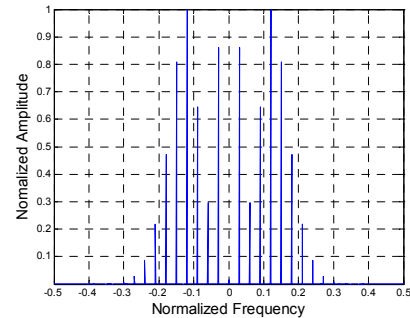


Fig. 2. SFM signal spectrum without noise.

#### 3.3. New algorithm

We are excited to find out that the spectrum bears some resemblance with a pulse train, irrespective of the amplitudes, and therefore are inspired to apply the PRI transform to the detection and estimation of SFM signals.

The resulting algorithm is described as follows.

Step1: Conduct the Fourier transform to obtain the signal spectrum;

Step2: Detect harmonic components whose strength is over a threshold;

Step3: Convert the spectrum to a pseudo-pulse-train (0-1 sequence) according to the detection results;

Step4: Perform the PRI transform;

Step5: Compare the resulting peaks with a threshold to decide if there is any SFM signal, and the locations of the over-threshold peaks provide the estimation of modulation frequencies.

Note that two thresholds are required. The threshold in Step5 is provided by the PRI transform itself [7], while the one in Step2 can be obtained by the constant false alarm rate (CFAR) technique. The algorithm can concentrate all the frequency components into a single peak, and is also suitable for multiple components with different modulation frequencies since the PRI transform can in itself estimate PRIs of interleaved pulse trains.

### 3.4. Discussion

#### 3.4.1. Estimation precision

PRI bins are utilized for calculating the PRI transform, and as a result the estimation precision mainly lies in the width of the PRI bin containing the peak. Also, PRI bins are not necessary to have the same width.

#### 3.4.2 Limitation to the number of harmonics

The PRI transform depends on a large number of pulses and thus the harmonics should be numerous enough, but there is not a quantitative norm. From (7), the larger the modulation index  $A$  and the smaller the wavelength, the better for applicability of our algorithm.

#### 3.4.3 Computation complexity

Let us estimate the number of floating point operations (FLOPs) of the algorithm. For a range cell, our algorithm mainly consists of a fast Fourier transform (FFT) and a PRI transform. A FFT of length  $N_a$  requires  $5N_a \log_2 N_a$  FLOPs [8], while a PRI transform needs less than  $C_{N_a}^2$  times of complex addition (see (3)), that is  $2C_{N_a}^2 = 2N_a(N_a - 1)/2 \approx N_a^2$  FLOPs. Therefore the total FLOP number is not more than  $5N_a \log_2 N_a + N_a^2$ . By comparison, the autocorrelation method, which also first need a FFT, requires  $5N_a \log_2 N_a + 2N_a^2 - 2N_a + 1$  FLOPs, the proving of which is omitted. Evidently our algorithm has lower computational load.

#### 3.4.4 False alarm (FA)

The information that our method explores is the frequency difference between different peaks from the spectrum without using the amplitude information. The performance will be jeopardized. For example, if we have signals of 10Hz, 20Hz and 30Hz of same power or not, then it might be recognized as a SFM signal. This situation will lead to many FAs. However, this is just a special case.

## 4. TEST RESULTS

We conduct the following experiments using simulated data, for testing the performance of the algorithm. The simulated signal consists of one or two components. The signal time is 2s (from -1s to 0.998s), the sampling interval is 0.002s, and thus its total length  $N_a$  is 1000. For Component1,  $\omega_{m1} = 2\pi f_{m1} = 2\pi \times 15 \text{rad/s}$  ; for Component2,  $\omega_{m2} = 2\pi f_{m2} = 2\pi \times 1 \text{rad/s}$ . The other parameters are the same:  $A = 5.5$ ,  $\phi_0 = 135^\circ$ . Fig. 3 displays the short-time Fourier transform (STFT) and the spectrum of Component1. From Fig. 3(a) it can be seen that the signal exhibits a sine shape, though contaminated by noise, implying the sinusoidal phase modulation. Its spectrum shows equal-spaced lines (Fig. 3(b)).

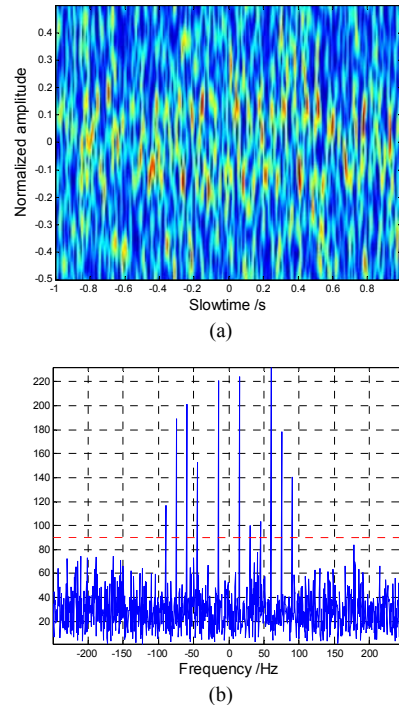


Fig. 3. Signal time-frequency distribution and spectrum under  $\text{SNR}_m = -5\text{dB}$ . (a) STFT; (b) Spectrum.

Under -5dB SNR, the signal is detected and estimated with the proposed algorithm, they are also estimated by the autocorrelation method for comparison. The results for a single component are shown in Fig. 4. We can see that both of the methods provide accurate estimations for the true vibration frequency 15Hz. The subharmonic components corresponding to sub-pulse-trains are suppressed after the PRI transform (Fig. 4(a)), but the autocorrelation function exhibits multiple peaks (Fig. 4(b)) which tends towards incorrect estimations (the error is multiple times of the true frequency), and this is also why the autocorrelation method is not usually used for detection.

The results for two targets are shown in Fig. 5. Clearly, the detection of the two vibrating targets is impossible from the autocorrelation function (Fig. 5(b)), let alone correct estimation. In contrast, from the results output by the algorithm (Fig. 5(a)) we can clearly find there are two vibrating targets above the threshold; the locations of the two peaks are near the true values, 11Hz and 15Hz, respectively.

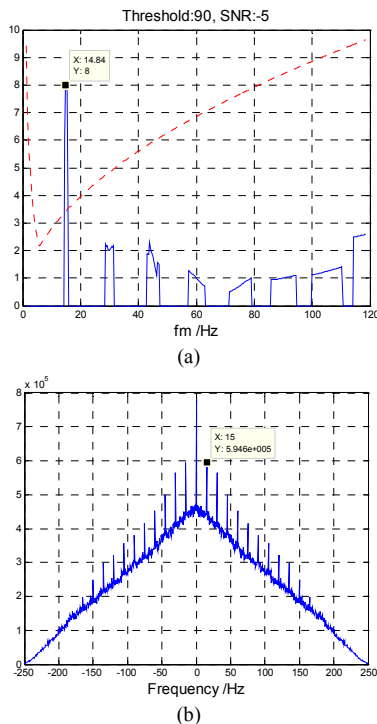


Fig. 4. Detecting/estimating results for a single component. (a) Our algorithm; (b) Autocorrelation method.

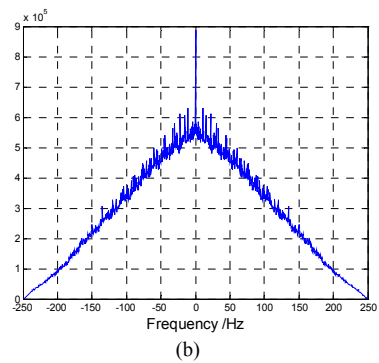
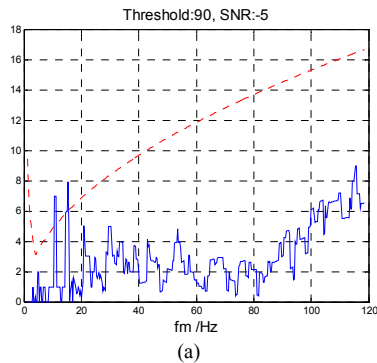


Fig. 5. Detecting/estimating results for two components. (a) Our algorithm; (b) Autocorrelation method.

For further performance analysis, we also plot the relationship between FA and the threshold used in Step4 when vibration is not present, as Fig. 6 shows. Five hundred times of Monte-Carlo simulations are performed. Clearly the FA decreases with increasing threshold on the whole, and it reaches 0.002, which is used in the following CFAR detection, when the threshold equals 90. In reality the threshold should be found by the given FA and the estimated noise covariance.

Keeping the FA rate constant (0.002 herein), we plot the probability of detection (PD) versus SNR curves for one and two targets respectively, as Fig. 7 shows. For one component, the PD is near one when the SNR is above -5dB, but still acceptable when it's above -10dB. The detection performance deteriorates when the component number increases since the SNR in the plot corresponds to the total energy and therefore the SNR for either component is in effect smaller.

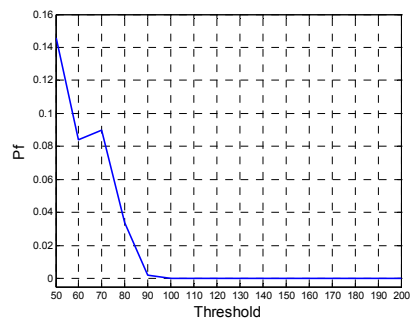


Fig. 6. FA rate versus threshold.

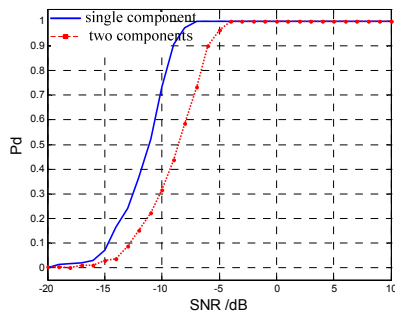


Fig. 7. Detection rate versus input SNR.

Fig. 8 plots the curve of Root-mean-square (RMS) error with respect to the SNR for evaluating the estimation performance. The true value of the modulation frequency is 15Hz. We can find the error decreases as the SNR increases on the whole. We can also see that, only when the SNR is above -5dB can the acceptable error be obtained. That is, the estimation requires higher SNR than does the detection. When the SNR is below -5dB and above -10dB, the estimation error is large but the PD is still relatively high. From this point we can presume that, in such a case, the peaks may be at incorrect locations though the algorithm has detected micro-motion targets with a high PD.

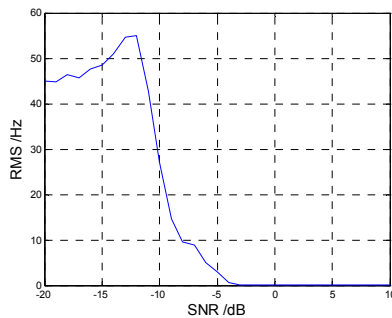


Fig. 8. RMS error for the modulation frequency estimation of Component1.

## 5. CONCLUSION

In this paper we have developed a PRI transform based algorithm for detecting SFM signals and for estimating the modulation frequencies. The key idea is to treat the signal spectrum as a pulse train and then to apply the PRI transform to the pseudo-pulse-train. The algorithm takes full advantage of the PRI transform so that it can detect multiple SFM signal components, while dispensing with the error of multiple-times of vibration frequencies facing the conventional autocorrelation method. It's not vulnerable to part-of-spectrum-peaks' missing, and doesn't require rigidly equal space between peaks since PRI transform can process pulse jitter. Also, the algorithm has lower computational load than the autocorrelation method. Simulated data have

demonstrated its performance. In our later work, we will use real SAR data to further test its performance.

## 6. REFERENCES

- [1] B. Deng, G. Z. Wu, Y. L. Qin, H. Q. Wang and X. Li, "SAR/MMTI: an extension to conventional SAR/GMTI and a combination of SAR and micromotion techniques," in *Proc. IET-RADAR*, 2009, pp. 42-45.
- [2] S. Krishnan and R. M. Rangayyan, "Detection of nonlinear frequency-modulated components in the time-frequency plane using an array of accumulators," in *Proc. IEEE-SP*, 1998, pp. 557-560.
- [3] P. Setlur, M. Amin and F. Ahmad, "Analysis of micro-Doppler signals using linear FM basis decomposition," in *Proc. SPIE*, 2006, pp. 1-11.
- [4] T. Thayaparan, S. Abrol, E. Riseborough, L. Stankovic, L. D. Lamothe and G. Duff, "Analysis of radar micro-Doppler signatures from experimental helicopter and human data," *IET Radar, Sonar and Navig.*, vol.1, no.4, pp. 289-299, 2007.
- [5] P. Setlur, M. Amin and F. Ahmad, "Optimal and suboptimal micro-Doppler estimation schemes using carrier diverse Doppler radars," in *Proc. ICASSP*, 2009, pp. 3265-3268.
- [6] N. S. Subotic, B. J. Thelen and D. A. Carrara, "Cyclostationary signal models for the detection and characterization of vibrating objects in SAR data," in *Proc. ACSSC*, 1998, pp. 1304-1308.
- [7] K. Nishiguchi and M. Kobayashi, "Improved algorithm for estimating pulse repetition intervals," *IEEE Trans. Aerosp. Electron. Syst.*, vol.36, no.2, pp. 407-421, 2000.
- [8] I. Cumming and F. Wong, *Digital processing of synthetic aperture radar: algorithms and implementation*, USA: Artech House, 2004.